OPERATIONAL EVALUATIONS OF NEW RADIAL GATE DESIGN

John A. Replogle[1]
Rick Adler
Robert S. Gooch

ABSTRACT

Radial gates have been used for decades because the force to operate them does not change much with water depth against the gate, albeit this force must overcome the constructed weight of the gate and the seal friction, usually with large electric motors. Typical radial gates offer only orifice flow under the gate and measuring flow rate with them has met with variable success. A recent modified gate design relocates the gate hinges and reduces the gate radius enough to allow the gate to rotate completely past a canal bottom seal so that the gate can operate both in an overflow weir mode and in a traditional underflow mode. The bottom seal and side seals are mounted on the channel floor and walls respectively. The gate bottom is rounded with a half-pipe in an attempt to standardize the exit jet in the hopes of improving and simplifying its hydraulic behavior for all openings. The weir blade is hinged to the gate top so it can rotate and remain vertical regardless of gate opening. This new design is counter-weighted so that it can be rotated with a small motor. The modifications to both the top and bottom of the gate should provide an estimated improvement in measurement accuracy to within ±2%, in the weir mode, and ±4 %, in the orifice, or undershot, mode. The design handles both floating and bed load debris because of the two flow modes.

INTRODUCTION

Radial gates have been used for decades primarily because they require about the same force to raise them at any opening within their range, albeit this raising force is often large enough to require powerful motors. They then typically use their own weight for closing. They traditionally offer only one mode of operation. The flow goes under the gate as orifice flow and into one of three environments, namely, free flow, transition-zone flow, or submerged flow. Attempts to accurately measure discharge rates with these gates have met with limited success, partly because the lip seals are variable. Many of the flows are in the transition zone that responds poorly to accurate computational procedures.

Provision for useful weir flow is not traditionally provided. Weir flows are expected to control upstream levels more easily and reliably by passing flow

---

[1] Research Hydraulic Engineer, US Water Conservation Laboratory, Phoenix, Arizona 85040; Principal, RSA Environmental, Inc., 1573 Mimosa Court, Upland, California 91786; and Civil Engineer, Salt River Project, Phoenix, Arizona, respectively.

variations downstream than can be accomplished with underflow orifices. This capability is particularly useful in manual operating mode, because small orifice openings in undershot gates tend to clog, and may require expensive depth sensors and automation to achieve the same level of performance.

A recent gate design attempts to address many of these concerns by raising the gate hinges or reducing the gate radius, such that the gate can be rotated though the bottom so that it can operate both as an overflow weir and as a traditional underflow gate. Figure 1 shows such a gate in a test channel at the Salt River Project, Phoenix, Arizona. The diagram of Figure 2 further illustrates the concept.

DESIGN CHANGES FROM TRADITIONAL RADIAL GATE

The manufacturer's overall design objective was to produce a control gate that was essentially a drop-in replacement for existing control structures from check boards to typical radial gates, offered to the user as a "turn-key" installation, providing reliable flow metering without field calibration, and equipped ready to interface with canal control software. Some of these objectives are still in development.

Figure 1. Counterbalanced gate.

Design features address several field operational issues such as trash handling and new gate installations "in the wet." Also planned, but not included on the test prototype, is the ability to replace gate seals, again "in the wet." Software packages to interface with canal operational software are also part of the system still being developed.

The bottom seal is moved from the traditional location on the bottom edge, or lip, of the radial gate to the channel floor, and the side seals are moved from the right and left edges of the gate to the channel walls. The weir blade, which is 75 mm (3 in) high on the tested prototype, is hinged to the gate top so it can rotate and remain vertical regardless of gate position.

The bottom of the gate is fitted with a half pipe about 160 mm (nominal 6-in pipe) in diameter to accommodate passing over the bottom seal and to standardize the exit jet in the hope that more convenient and reliable discharge relations will result than those for traditional radial gates. The modifications to both the top and bottom of the gate are attempts to maintain measurement accuracy to within ±2 %, in the weir mode, and ±4 %, in the orifice, or undershot, mode. The entire gate is counter-weighted to minimize the motor-size requirements. Traditional radial gates, as previously mentioned, depend on the gate weight to close, and usually use cables for opening. Because of the weir flow requirement, and the counterweights, positive drive to both open and close the new gate design is provided with gear drives or linear actuators, depending on gate size.

In underflow mode, there frequently is a transition zone that responds unreliably to both the free-flow equations and to the submerged flow equations. When this zone is identified, it should be possible to adjust a gate to avoid the zone. This would appear to be more readily accomplished when two or more parallel gates are installed, and where the flow can be apportioned between weir flow and undershot flow to avoid a troublesome transition zone.

The trash handling features should be enhanced by the ability to pass floating trash in the weir mode, and to pass bottom sediments in the typical radial-gate, under-shot mode. When parallel gates are employed, operating one gate in weir mode and the other in undershot mode can often satisfy flow requirements. The gate-flow modes potentially can be alternated periodically without causing a flow surge in the canal.

Only the general hydraulic behavior of the gate was tested. The hydraulic design features aim to improve the measurement accuracy of flows that are perhaps as small as 2% or 3 % of the maximum flow through the gate. This can be accomplished using the weir overflow mode for the low flows. The undershot mode operates best in the range greater than about 5% of maximum flow.

THEORY OF OPERATION

Figure 2 illustrates the method used to compute the flow area of the radial gate opening, where L is the radius of the gate arc from the upstream gate face to the center of pivot; D is the diameter of the bottom half-pipe fitted to the gate; W is the gate opening without the half-pipe attached to the bottom, W_n is the net gate opening with the half-pipe in place. A 0° closure occurs when the bottom-most point of the attached half-pipe is centered on the seal. The “seal-offset” is assumed to be 35 mm (1.375 inches) above the floor with 3 mm (1/8 inch) of deflection. This seal offset can be adjusted in the field.

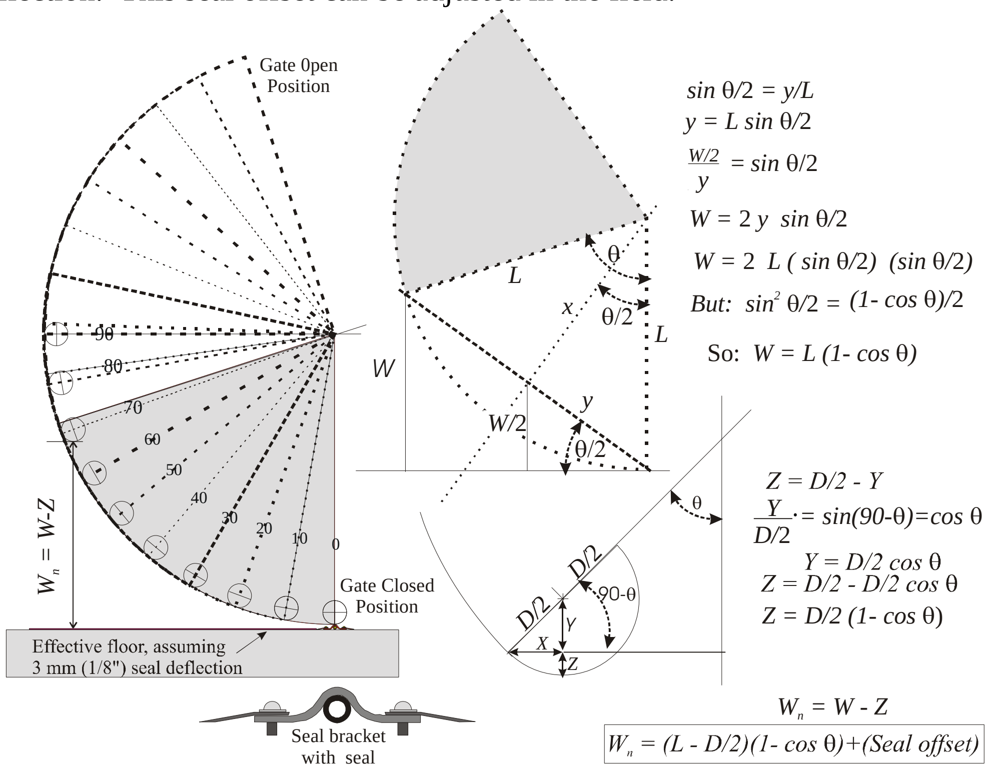

Figure 2. Computation scheme for determining effective gate opening.

The net opening, W_n, as derived in Figure 2 is:

$$W_n = \left(L - \frac{D}{2}\right)(1 - \cos\theta) + (Seal\,Offset) \qquad (1)$$

and the inverse for any angle, θ, is:

$$\theta = \cos^{-1}\left(1 - \frac{W_n - Seal\,Offset}{L - \left(D/2\right)}\right) \qquad (2)$$

It is probable that the gate opening may not be hydraulically valid for positions where the bottom seal can interfere. This interference distance is estimated to be at a gate-arc-opening that would produce a bottom-of-gate position from the seal center of about five times the seal height, or about 200 mm (8 in), which calculates to be about 6° of rotation from closed. This rotation would produce an opening for this test gate of about 48 mm (1.9 in) for a seal height of 40 mm (1-5/8 in), and is just beyond the beginning of the seal hold-down plate.

Discharge Equation for Underflow

Assuming the flow in half of a rectangular jet, using the floor as the line of symmetry for the image, and with width *B*, (into the page, Figure 3), we can write the Bernoulli energy equation between points 1 and 2, getting:

$$\alpha_1 \frac{V_1^2}{2g} + h = \alpha_2 \frac{V_2^2}{2g} + C_c W_n + h_f \qquad (3)$$

where α_1 and α_2 are the velocity distribution coefficients in the plane of flow at points 1 and 2 respectively; V_1 and V_2 are the average velocities in the same planes; C_c is the contraction (or expansion) coefficient applied to the computed net gate opening, W_n, to obtain the free flow jet thickness, y; g is the acceleration due to gravity; and h_f is the energy lost between the two planes, which we will represent as a function of the energy head at location 2, or $h_f = k\, V_2^2 /2g$.

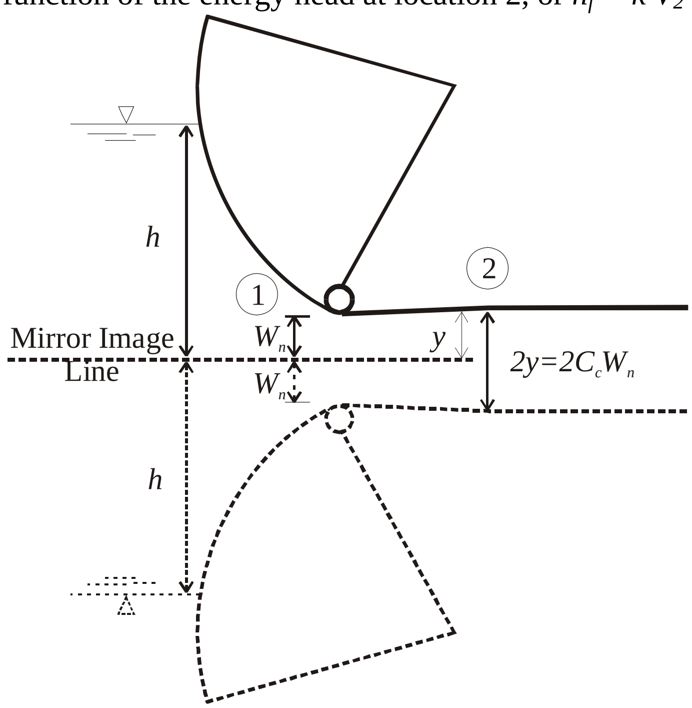

Figure 3.

By continuity, $V_1 = Q_T/A_1$ and $V_2 = Q_T/A_2$, where Q_T is the total double flow of Figure 3, and A_1 and A_2 are the flow cross-sectional areas in the plane of flow at points1 and 2, Figure 3. Substituting.

$$\frac{\alpha_1}{2g}\left(\frac{Q_T^2}{A_1^2}\right) + h = \frac{\alpha_2}{2g}\left(\frac{Q_T^2}{A_2^2}\right) + C_c W_n + \frac{k}{2g}\left(\frac{Q_T^2}{A_2^2}\right) \tag{4}$$

Solving first for $(Q_T)^2/2g$,

$$\frac{Q_T^2}{2g} = \frac{h - C_c W_n}{\left(\frac{\alpha_2 + k}{A_2^2} - \frac{\alpha_1}{A_1^2}\right)} \tag{5a}$$

Then rearranging,

$$Q_T = \frac{A_1 A_2}{\sqrt{(\alpha_2 + k)A_1^2 - \alpha_1 A_2^2}} \sqrt{2g(h - C_c W_n)} \tag{5b}$$

but $A_1 = 2\ Bh$, and $A_2 = 2\ BC_cW_n$, so,

$$Q_T = \frac{(2Bh)(2BC_c W_n)}{\sqrt{(\alpha_2 + k)(2Bh)^2 - \alpha_1 (2BC_c W_n)^2}} \sqrt{2g(h - C_c W_n)} \tag{6}$$

Now, the discharge for half of the imaged opening is $Q = Q_T/2$, and

$$Q = \frac{Bh(C_c W_n)}{\sqrt{(\alpha_2 + k)h^2 - \alpha_1 (C_c W_n)^2}} \sqrt{2g(h - C_c W_n)} \tag{7}$$

Equation 7 is expected to describe the flow for a free-discharging gate. The values for the velocity distribution coefficients, both α_1 and α_2 are expected to be between 1.005 and 1.02, and *k* is estimated to be approximately 0.01, or about 1% of the exit velocity head. The contraction (expansion) coefficient is the main contributor to the variation in evaluating the equation. Because of the converging curvature of the gate and the rounded edge, the C_c value can be expected to approach or exceed a value of 1.0 much as a circular, diverging nozzle with a rounded entrance, (Brater and King, 1982). They quote Freeman=s results showing C_c to be as great as 2.0. Because this is a rectangular opening instead of circular, and the nozzle in this case is short, the equivalent value may be on the order of 0.75 to 1.5, and may vary with the gate opening according to a function to be determined experimentally. Alternatively, the radius of curvature can be expected to produce near parallel flow near the exit and the value of C_c would then be 1.0. However, the flow around the circular exit may create a vacuum, (as yet not verified for the flows tested) and this may require an adjustment in head rather than the process of adjusting flow opening with C_c.

For a submerged orifice-type flow situation, the eddy and sidewall-friction energy losses can be assigned to the value of h_f determined by experiment.

<u>Discharge Equation for Weir Flow</u>

For the sharp crested over fall weir the appropriate Equation is (Bos, 1989)

$$Q = C_e \frac{2}{3}\sqrt{2g}\; b_c h_w^{1.5} \tag{8}$$

where h_w is the head over the weir measured at an appropriate distance upstream of at least 3 or 4 times the maximum h_w value, b_c is the width of the weir opening, and C_e is an effective discharge coefficient, which is a function of h_w/p and the channel-width to weir-width ratio. If the width ratio were unity for this gate, C_e would be described by (Bos, 1989):

$$C_e = 0.602 + 0.075\frac{h_w}{p_1} \tag{9}$$

The factor p_1 is the height of the weir crest above the channel floor. As constructed, the gate has a seal near each end that causes the effective width of the weir to be less than full width by 7.5 %. Future designs plan to place the seals in a wall recess that will allow full width flow. However, the current edge seals appear to be just far enough upstream from the blade to prevent the flow from contracting from the sides by the time the flow reaches the weir blade and causes the flume over fall to appear to be that of a suppressed weir of width equal to the remaining clear span. Thus, Equation (9) is expected to apply to the net width of 1.41 m (4.62 ft).

In the test situation, the gate was mounted in a containment box, and the head was detected near the box entrance, which was closer to the weir over fall than is usually recommended. This meant that a depth detected further upstream, might be slightly greater. To adjust the current tests to standard weir equations, at least two approaches can be considered. One is a correction value, Δh_w, added to h_w (which may also be applied to the orifice modes) because Equation 9 may not fully account for the velocity of approach. Another approach is to directly increase C_e.

DESCRIPTION OF TEST FACILITIES

A rectangular channel in an outdoor research facility at the Salt River Project, Phoenix, Arizona, was adapted for the gate study (Figure 4). The channel was approximately 1.83 m (6 ft) wide, 2 m (6.75 ft) deep, and 23 m (75 ft) long. A sluice gate controlled the water supply from a small header pond. Pond level was maintained with an overspill weir that was approximately 3 m (10 ft) wide. Because of the relatively short lengths, special efforts were required to baffle the inflow to the test gate and then to recondition the flow downstream of the gate for discharge measurements with a rectangular long-throated flume.

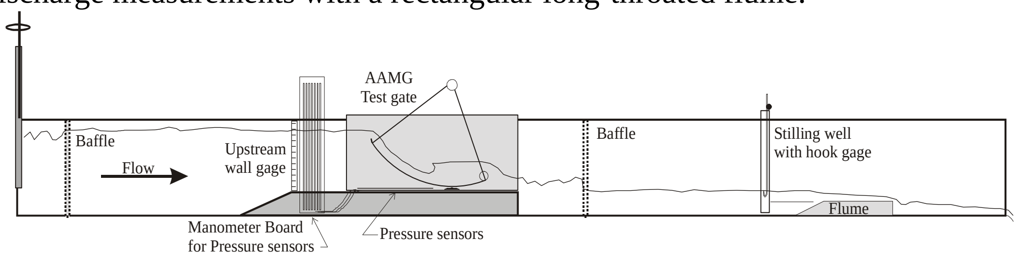

Figure 4. General layout of the facility for the AAMG test gate, shown here in the overflow, or weir mode.

Water was supplied from a canal above the facility and returned to a canal below the facility. The available flow rates were generally about 0.4 m^3/s (15 cfs) with occasional access to 1.2 m^3/s (40 cfs). While this was adequate for the weir flow function, it was only enough to test about the lower one-third of the expected underflow operation.

The discharge rates were determined with the long-throated flume. The depth over the flume was read with a hook gage in a 15 cm (8 in) diameter stilling well that sensed the depth upstream of the flume through a group of drilled holes in a 25 mm (1 in) plastic pipe placed on the channel floor against one of the approach walls and connected to a stilling well with about 4 m of 8 mm (5/16 inch) plastic tubing.

Because of the difficulty of installing floor taps for detecting the pressures under the gate, a 20 mm (3/4 in) hard copper tube was fitted with a series of smaller, 8 mm (5/16 in) copper tubes that were placed inside the larger tube and curved out through holes in the larger tube, soldered into place, and ground off smooth with the outer surface of the larger tube.   These holes were spaced at spaced at 305 mm (12 in) intervals (approximately at locations indicated by the x-values of the data points in Figure 7). These holes produced pressures similar to floor taps. These small copper tubes were connected to a manometer board with plastic tubing.

PRESENTATION OF DATA

The underflow condition is the traditional way that typical radial gates are operated. Five gate openings ranging from 68 mm to 296 mm (2.6 to 9.73 in) and discharge rates from about 0.2 m^3/s to 1.25 m^3/s (8 cfs to 45 cfs), were used.

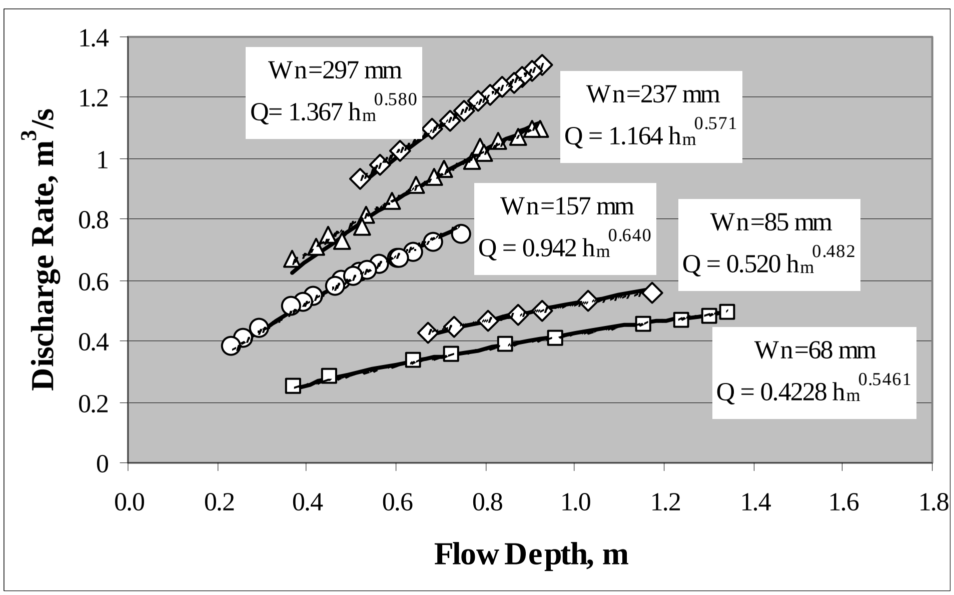

Figure 5. Undershot flow. Curves are fitted by selecting C_c values for use in Equation 7 for each gate opening.

Figure 5 shows the field laboratory data for the various orifice openings of the gate, W_n. Observation of the discharge jet showed that the seal on each side shadowed the opening reducing it by the seal intrusion of 38 mm (1.5 in) on each side for a net orifice width of 1.397 m (55 inches).   If we choose a C_c for each data set for use in Equation 7, the computed curve fit seems adequate, and these curves are plotted in Figure 5 as heavy solid lines. The statistical-trend lines to the data, with their equations, are shown as thin dashed lines. These choices for C_e appear to follow an approximate linear pattern, as shown in Figure 6.

Other adjustments were attempted, one based on the presumption of negative pressures under the gate at small openings. This possibility is supported from the floor pressure readings, Figure 8, for a gate opening, W_n = 85 mm, which shows a slight positive pressure on the curved bottom of the gate beyond the lowest point, and a lower pressure after leaving the gate, presumably caused by the curvature of the bottom, and then an increase to what may be a standing wave and ultimately to parallel flow and hydrostatic pressure downstream. Somewhere in this region, a value of Cc slightly greater than 1 finds support. If a useable negative pressure does exist, a consistent relation to gate opening was not found.

Finally a correction based on a Reynolds Number using the hydraulic radius of the orifice opening and various other lengths as the characteristic length, was tried with similar disparity. The more simple adjustment of C_c is thus used in this presentation.

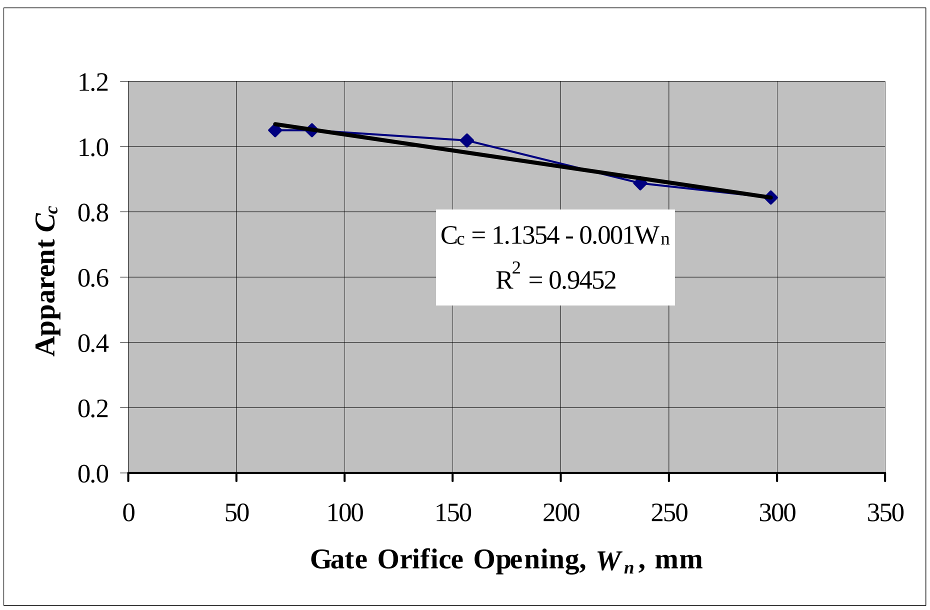

Figure 6. Apparent contraction coefficient, C_c, which is needed to approximately fit data to Equation 7.

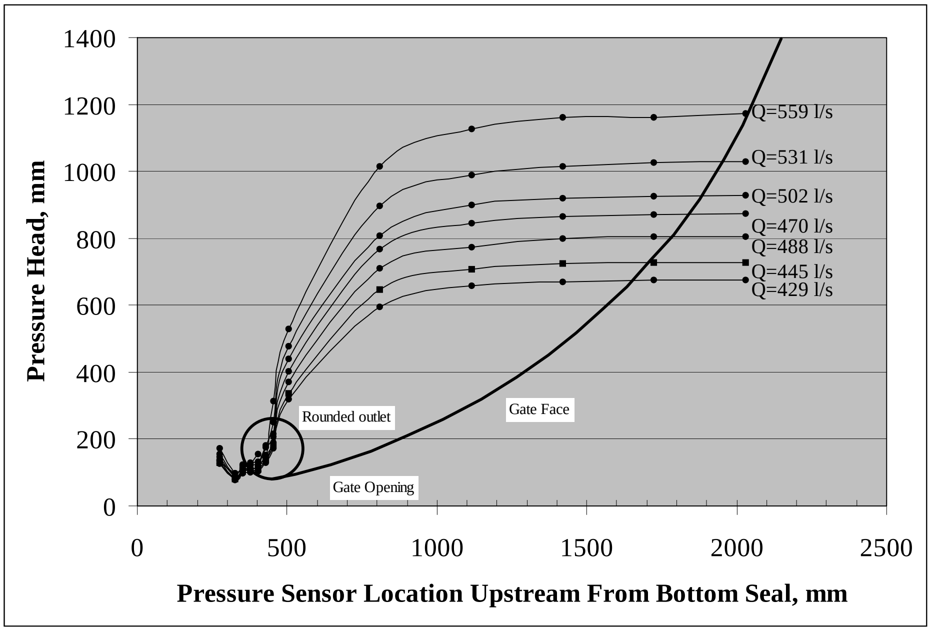

Figure 7. Pressure readings under gate with opening, W_n=85 mm (3.3 in), are shown in relation to rounded bottom of gate and the upstream gate face.

In weir flow, h_w should not approach five times the value of the weir height above the channel floor, $p_{1,}$ because at that point, the upstream flow may be at critical depth, and the weir would not be a flow control (Bos, 1989). Thus, in any canal that has a maximum upstream depth of flow, there is a practical limit to how far down the gate can be rotated for weir flow. For example, if the canal depth limit is 1.5 m (5 ft), then any weir edge should stay above 0.3 m (1 ft), leaving a maximum head of 1.2 m (4 ft) at maximum upstream canal depth.

However, in canals where this gate is likely to be installed, the downstream canal depth is likely to control weir limits, and the downstream depth may usually be limited to something approximating the value of the head over the weir, at which point the weir would start to submerge, or may already be submerged, depending on whether a drop in the downstream channel is provided.

The usual recommendation for weirs is that the downstream water surface not approach higher than about 50 mm (2 inches) below the crest of the weir. This limit in this example would be about h_1=0.75m (2.5 ft). Equation 8 produces 1.25 m^3/s per meter width (13.5 cfs per foot) for this head. This is possibly an upper limit, near 50% of maximum flow recommended for the prototype gate, and would require special downstream channel conditions to even operate in weir mode. A more likely maximum operating head is about 0.4 m (1.3 ft), which, by Equations 8 and 9, is about 0.47 m^3/s per meter width (5 cfs per ft). These overflow weir-flow limits seem to agree with operational limits on overshot leaf gates and related types. In these gates, increased capacity is usually accommodated with wider structures.

When the field data is compared directly with Equations 8 and 9, an offset of about 10% is noted. Again the weir width was restricted at each end by the seals and the mechanical follower used to keep the weir vertical. The net width used was Modifying Equation 9 as follows:

$$C_e = 1.1\left(0.602 + 0.075\frac{h_w}{p_1}\right) \quad (10)$$

represents a good fit to the data, Figure 8. This modification is larger than the combined effects that would be covered by the recommendations of Kindsvater and Carter (1959) and by Bos (1989), which for this weir are to increase the effective head and decrease the effective width, each by 1 mm (.04 in).

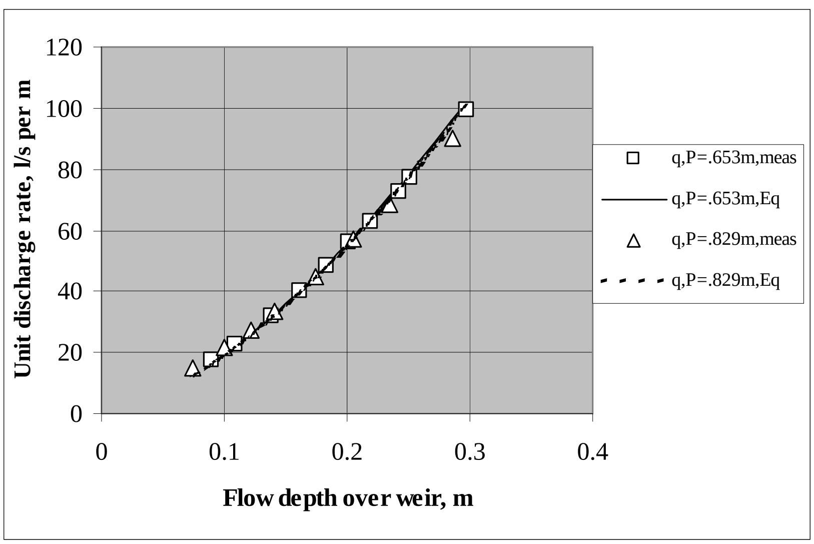

Figure 8. Curves as fitted to data using Equations 8 and 10.

Differences in C_e from that of the full height vertical weir case might at first be thought to relate to the reentrant nature of the curved gate below the 75 mm (3 in) high weir blade. This could cause some back flow that would effectively require an increase in the head on the weir for a given discharge, but this would, in effect, be in the wrong direction, decreasing C_e.

Another explanation would be that the backflow causes a hydraulic roller, of sorts, that raises the main flow such that the effective p_1 is reduced to approximately the magnitude of the value for h_w. This would cause about a 10% increase in C_e, as calculated by Equation 8, and would match the data well.

CONCLUSIONS

The prototype gate appears fully capable of meeting operational requirements related to controlling and measuring flow rates in both overshot (weir) and undershot (orifice) modes. This has yet to be fully established. The overshot mode provides a near constant upstream canal level while passing a small flow downstream, even in manual mode. The same upstream control behavior could conceivably be accomplished with a traditional radial gate or in the undershot mode of this new gate, provided the depth detection and motor operator are suitably designed, but clogging at small openings is a bothersome field problem. With the usual margin of error on canal level detection, the weir mode would be expected to better hold the upstream level than the undershot mode, while the undershot mode would be expected to deliver more constant downstream flows.

One of the design objectives was to provide measurement accuracies to within ∀2% for weir flow and ∀4% for undershot (orifice) flow. These limited tests showed that this prototype displayed measurement repeatability near or within these values. Further testing is required.

The weir flows behaved nearly as expected, but at about a uniform 10% more discharge for a given head than that for a standard vertical weir, and appear to be repeatable to within the objective of 2% usually obtainable with weir flows. This deviation is speculated to be due to the back-tilting nature of the circular gate face presented to the approaching flow that perhaps supports the approach flow in a manner that mimics a high floor level that would produce an appropriate increase in C_e. This was not proven. However, the C_e values seem to be reasonable and otherwise in line with previous studies, when using the stated adjustment in C_e.

When canal flow rates exceed the tolerance limits for weir flow, the gate can be rotated to the underflow mode. Thus, this structure can accommodate a wide range of flows in a restricted width that would challenge simple overflow devices.

Trash, of both floating and bed load varieties, appear to be readily handled by the dual modes of operation and particularly by parallel installations that can allow mode switching between them with only minor surges in the downstream flow.

The undershot mode produced variable coefficients of contraction, C_c, that exceeded 1.0 at low openings, but at larger openings appear to be approaching the lesser values associated with traditional radial gates.

REFERENCES

Ackers, P., W.R. White, J.A. Perkins, and A.J.M. Harrison. 1978. Weirs and Flumes for Flow Measurement. A Wiley-Interscience Publication, John Wiley and Sons, New York. 327 p.

Bos, M.G. 1998. Discharge Measurement Structures. Publication 20. International Institute for Land Reclamation and Improvement/ILRI. P.O. 45, 6700 AA Wageningen, The Netherlands. 401 p.

Brater, Ernent F. and Horace Williams King. 1982. Handbook of Hydraulics. McGraw-Hill Book Company, New York. 604 p.

Horton, Robert E. 1907. Weirs Experiments, Coefficients, and Formulas. Water-Supply and Irrigation Paper No. 200, Series M, General Hydrological Investigations, 24, United States Geological Survey. 195 p.

Kindsvater, Carl E. and Rolland W Carter. 1959. Discharge Characteristics of Rectangular Thin-Plate Weirs. Paper No. 3001. Transactions of the American Society of Civil Engineers. Volume124, pp 772-822.

Errata from Previous Versions): Corrected Eqs: Errors in Equations and in typing. Negative sign before h_f changed to Plus sign. This results in a minor change in computations with Equation 7.

Figures and data updates: This included some new data and corrections in the spreadsheet when converting units of measure.

Conclusions changed due to data updates.